NAA-SR-1921

1

PHYSICS AND MATHEMATICS

UNITED STATES ATOMIC ENERGY COMMISSION

THE THEORETICAL CALCULATION OF THE ATTENUATION OF GAMMA RADIATION FROM A SWIMMING POOL TYPE REACTOR

By
R. L. Ashley
D. S. Duncan

August 15, 1957

Atomics International Division
North American Aviation, Inc.
Canoga Park, California

Technical Information Service Extension, Oak Ridge, Tenn.

2

LEGAL NOTICE

This report has been reproduced directly from the best available copy.

Printed in USA. Price $1.25. Available from the Office of Technical Services, Department of Commerce, Washington 25, D. C.

AEC Technical Information Service Extension
Oak Ridge, Tennessee

THE THEORETICAL CALCULATION OF THE ATTENUATION OF GAMMA RADIATION FROM A SWIMMING POOL TYPE REACTOR

BY:

R. L. ASHLEY
D. S. DUNCAN

ATOMICS INTERNATIONAL

A DIVISION OF NORTH AMERICAN AVIATION, INC.
P.O. BOX 309 CANOGA PARK, CALIFORNIA

CONTRACT: AT(11-1)-GEN-8
AUGUST 15, 1957

TABLE OF CONTENTS

		Page No.
I.	Introduction	7
II.	Description of the Reactor Core	8
III.	Gamma-Ray Spectrum	9
	A. Gamma Rays From the Reaction U^{235} (n, f)	9
	B. Gamma Rays From the Reaction U^{235} (n, γ)	11
	C. Gamma Rays From U^{235} (n, f) and U^{235} (n, γ)	11
	D. Capture Gamma Rays From Hydrogen	11
	E. Capture Gamma Rays From Aluminum	11
	F. Decay Gamma Rays From Al^{28}	12
	G. Gamma Rays From Fission Products	12
IV.	Description of the Attenuation of the Radiations	13
	A. Core Radiations	13
	B. Shield Capture Gamma Rays	17
V.	Linear Absorption Coefficients and Buildup Factors	24
VI.	Calculation of the Dose Rate	29
VII.	Comparison of Calculated and Measured Values	31
VIII.	Discussion	32
	A. Uniform Power Density and Average Thermal Neutron Flux	33
	B. Fission Product Gamma-Ray Spectrum	33
	C. Dose Buildup Factors	34
	D. Geometry	35
	E. Shield Density	36
IX.	Conclusion	37
	References	39

ABSTRACT

In order to determine the adequacy of the calculational methods employed by Atomics International to solve shielding problems on such reactor systems as the SRE and OMRE, it is required that the results obtained by using these methods be compared with accurate experimental information. Since the only reactor on which such experimental data[1] is available is the Oak Ridge Bulk Shielding Reactor, the theoretical attenuation of gamma radiation in the BSR shield was evaluated. The results were compared with the measurements of the gamma-ray attenuation from this reactor out to a distance of 700 cm from the core. The analysis performed indicates that it is possible to reproduce the measured data quite accurately over the entire range of water thickness for which measurements have been made, the average value of the calculated to measured dose rates being 1.25 with the maximum deviation from this value being less than 19 per cent. The formulation and assumptions necessary in the analysis are discussed. It is concluded that the spectra and method used will yield results which are more than adequate when dealing with shielding analyses, per se, and are probably adequate for heat generation problems as well.

INTRODUCTION

There are many reactor designs which are similar to the Oak Ridge Bulk Shield Reactor (BSR) but in which the core loading or specific design is sufficiently different to limit the direct application of the BSR experimental dose rate measurements[1] to shield design. This is caused by several factors: the core may contain more fuel than used in the measurements; hence, for the same reactor power the average thermal neutron flux in the fuel will be less; or the metal to water volume ratio may be different, in which case the gamma-ray linear absorption coefficient of the core will change, thus changing the amount of radiation leaking into the shield. Such changes as these will reflect themselves in both the shape and magnitude of the thermal neutron flux in the shield. Also, any change in core materials e. g., substitution of steel or zirconium for aluminum, would certainly change the core gamma-ray source. Any of the changes or variations noted would permit only the limited utilization of the experimental data[1] reported.

Even when the core design is similar, it may be desirable to know the magnitude of heat generation in the surrounding shielding. In this case the calculation must deal with the gamma-ray spectrum being generated in the core and shield. Since the BSR gamma-ray measurements were of dose rate, they are of no direct use in heat generation calculations. Other problems will undoubtedly arise in which the answer can be achieved only by direct calculation, rather than by manipulation of the experimental data.

This report considers the core and shield gamma-ray spectra and describes a method for determining the gamma-ray dose rate at any distance in the shield. The spectra required for the determination of the core gamma-ray source were not clear; several choices were available. For example, the spectrum of prompt fission gamma rays[2, 3, 4] is still in question. Similarly, the form of the spectrum generated during radiative capture in U^{235} has not been specified with certainty, nor has the spectrum generated by fission products during reactor operation[5] been defined with complete certainty. However, a choice of spectra based on the work of Bertini et al., [6] is made for these three cases and is utilized throughout the analysis.

In the calculations the shield capture gamma-ray dose rate was also evaluated. The fact that the total calculated dose rate (due to both core and shield capture gamma rays) fits the Oak Ridge BSR measurements so well indicates that the spectra chosen for the core radiations and the methods and assumptions used in evaluating the dose rate in the shield were quite reasonable. It is belived that this spectrum and calculational method will prove of assistance in shielding and heat generation calculations for other types of reactors as well as for the particular type analyzed in this report.

In the analysis of the dose rates from the core radiations, the gamma-ray dose buildup factors[7] were fitted to a simple exponential, while in the analysis of the dose rates from shield capture gamma rays, the dose buildup factors were fitted to a quadratic. These expressions were then inserted into the integration describing the attenuation of the source radiations.

II. DESCRIPTION OF THE REACTOR CORE

The design of the type of reactor considered in this analysis has been described elsewhere[8] and will not be elaborated on here. The core of the reactor on which the measurements[1] were made contained 28 fuel elements with a total of 3.6 kg of U^{235}. In the analysis which follows, a value[8] of 0.70 for the ratio of the metal to water volume in the core was used. From this, it was found that the core contained 5.84×10^4 gm of water, 3.84×10^3 gm of uranium, and 1.096×10^5 gm of aluminum. The total volume of the core was found to be 9.92×10^4 $cm.^3$

The average thermal neutron flux in the uranium was calculated using the expression

$$\overline{\phi}_{th} = \frac{3.1 \times 10^{16} P}{\frac{N_o}{235} \times 10^3 \sigma_f M} \qquad \ldots (1)$$

where:

P = reactor power level (Mw)

N_o = Avogadro's number

σ_f = U^{235} fission cross section corrected to 63° C and for a Maxwellian distribution (cm^2)

M = mass of U^{235} (kg) .

With $\sigma_f = 478 \times 10^{-24} cm^2$, one obtains $\overline{\phi}_{th} = 7.02 \times 10^{12}$ $\frac{\text{neutrons}}{cm^2\text{-sec-Mw}}$.

This is actually the average thermal neutron flux in the uranium, and not in the reactor. However, for the particular reactor under consideration, it is not expected that the core averaged thermal neutron flux will vary significantly from this value. As a result, this value shall be used to represent the average thermal neutron flux in the core.

In most of the practical problems of shield design and heat generation, the details of the power distribution in the core are not known. Consequently, some assumption relating to this distribution must be made. The one which is the simplest and probably the most often used is that the power distribution in the core is uniform. This assumption will also be made in the analysis which follows. By doing so, it is hoped that the results obtained will help to justify its use in this problem, and problems of a similar nature, and also give some insight for the magnitude of the error involved.

III. GAMMA-RAY SPECTRUM

The sources of radiation considered in this analysis include the gamma rays generated in the following reactions: U^{235} (n, f), U^{235} (n, γ), H (n, γ), Al^{27} (n, γ), and $Al^{28} \rightarrow \gamma$, as well as those emitted by fission products. Gamma rays from inelastic scattering in aluminum[23] and uranium[6] as well as capture gamma rays from U^{238} are not considered due to their relatively low intensities. The spectra generated from each of the reactions considered in this analysis are discussed in the following.

A. GAMMA RAYS FROM THE REACTION U^{235} (n, f)

There is still some question concerning the spectrum from prompt fission gamma rays. Two early measurements[2, 3] appear to agree in the total energy available, but not in the average energy per photon. The data of Deutsch and

Rotblat[3] gives a total energy of 5.1 ± 0.3 Mev/fission and an average energy per photon of 1 Mev; whereas, Kinsey et al., give 4.6 ± 0.1 Mev/fission, and an average energy of 2.5 Mev. Another measurement,[9] reported at the Reactor Shielding Information Meeting in November, 1953, indicated a very pronounced peak at about 1 Mev, and no other strong lines appearing. A still more recent measurement was reported by Gamble[4] at Oak Ridge National Laboratory in June, 1955. From a curve of Gamble's data which plots photons/fission-100 kev as a function of gamma-ray energy over the range from 0 to 7.6 Mev, the spectrum can be approximated[6] by

$$N'_u(E) = 7.6e^{-1.01E} \text{ photons/Mev-fission} . \qquad \ldots(2)$$

The total energy released per fission and the average energy per photon are obtained as follows:

$$E_T = \int_0^{7.6} EN'_u(E)dE = 7.45 \text{ Mev/fission} , \qquad \ldots(3)$$

$$\overline{E} = \frac{\int_0^{7.6} EN'_u(E)dE}{\int_0^{7.6} N'_u(E)dE} = \frac{7.45}{7.52} = 0.991 \text{ Mev/photon} . \qquad \ldots(4)$$

Although the average photon energy appears to be in good agreement with previously reported measurements,[3,9] the total energy released per fission is considerably higher. However, preliminary data from measurements presently being made at Oak Ridge National Laboratory by Maienschein, Peele, and Love[10] tend to substantiate the total energy released per fission reported by Gamble. Consequently, it was decided to use the spectrum defined by Eq. (2) in this analysis.

B. GAMMA RAYS FROM THE REACTION U^{235} (n, γ)

When U^{235} captures a neutron producing U^{236}, the excess energy (neutron binding energy) will be emitted in the form of gamma rays. The neutron binding energy for this reaction is 6.426 Mev.[11] Very little information is available concerning the spectrum of this radiation; it has been conjected,[6] however, to have the same spectral distribution as that of the prompt fission gamma rays. Since the BSR is a thermal reactor, the ratio of the number of radiative captures to the number of fissions in U^{235} will be assumed to be equal[24] to 0.184. Thus, the spectrum from radiative capture may be approximated[6] by

$$N''_u(E) = 1.21e^{-1.01E} \text{ photons/Mev-fission} . \quad \ldots(5)$$

C. GAMMA RAYS FROM U^{235} (n, f) AND U^{235} (n, γ)

The spectrum of prompt fission gamma rays plus U^{235} capture gamma rays is, by addition

$$N_u(E) = 8.81e^{-1.01E} \text{ photons/Mev-fission} . \quad \ldots(6)$$

Thus, the total gamma-ray energy released per fission by U^{235} within discrete energy intervals is

$$E_{ab} = 8.81 \int_a^b E\, e^{-1.01E}\, dE \text{ Mev/fission} . \quad \ldots(7)$$

D. CAPTURE GAMMA RAYS FROM HYDROGEN

The capture gamma-ray spectrum from hydrogen is well known to be composed of a single line at 2.23 Mev, one photon being emitted per neutron capture.[12]

E. CAPTURE GAMMA RAYS FROM ALUMINUM

Detailed information on the capture gamma-ray spectrum of aluminum in the region above 2.7 Mev has been obtained by Kinsey and co-workers[13] and in

the region below 2.7 Mev by Braid.[14] The total energy accounted for was 7.8 Mev. For purposes of this calculation, the spectrum was divided into eleven energy intervals with a single representative energy chosen for each. The gamma-ray energy released per thermal neutron capture within these intervals was then obtained by summing up the individual contributions for each interval and normalizing, such that the total Mev per capture would be equal to the neutron binding energy (7.72 Mev).

F. DECAY GAMMA RAYS FROM Al^{28}

When aluminum absorbs a neutron the result is Al^{28} which is radioactive, having a half life of 2.27 minutes.[15] This isotope decays by emission of a beta particle and a 1.78 Mev gamma ray.[15] Since the half life is so short, it may safely be assumed that when the BSR measurements were taken, the Al^{28} activity was effectively saturated. Thus, this additional gamma ray was included in the analysis.

G. GAMMA RAYS FROM FISSION PRODUCTS

The fission product decay gamma-ray spectrum between 0.36 and 5.8 Mev reported by Peelle, Zobel, and Love[5] has been approximated[6] by

$$N_p(E) = 9.0\, e^{-1.33E} \text{ photons/Mev-fission} \quad . \qquad \ldots(8)$$

Thus the total fission product gamma-ray energy released per fission by U^{235} within discrete energy intervals is

$$E_{ab} = 9.0 \int_a^b E\, e^{-1.33E}\, dE \text{ Mev/fission} \quad . \qquad \ldots(9)$$

The spectrum given by Eq. (8) was based upon a fuel irradiation time of approximately 1 hour so that the decay gamma-ray activity of the long-lived fission products, i.e., those with half lives greater than several hours, was not considered. This is probably a good approximation to the exposure accumulated by the BSR fuel elements which had negligible fission product gamma-ray activity at

the time the measurements were begun.[1] Bertini, et al.[6], has shown that even though there exists an estimated probable error of ±20 per cent in this spectrum, it is still in very close agreement with the spectrum estimated by Way[16] after correcting the latter for the contribution from long-lived fission products.

The gamma-ray energy spectrum for the U^{235} (n, f) and U^{235} (n, γ) reactions, Eq. (6), was integrated over discrete energy intervals ranging from zero to 10 Mev, and the gamma-ray energy spectrum for the fission products, Eq. (8), was integrated over intervals ranging from 0.36 to 5.8 Mev. Wherever possible, these intervals were chosen so that their average energies would correspond to the specific energies used to represent the aluminum capture gamma-ray spectrum By so doing, it was possible to represent the entire gamma-ray energy spectrum of the core, over the range of energies considered, by 18 discrete energy lines with fairly uniform spacing. The result of the calculations for determining the gamma-ray source strength of the core, using these energy lines, is summarized in Table I.

IV. DESCRIPTION OF THE ATTENUATION OF THE RADIATIONS

A. CORE RADIATIONS

The dose rate at any position in the shield due to gamma radiation from the core may be described by the expression

$$D_\gamma = \int_V \frac{S_v B_r e^{-\sum_i \mu_i r_i}}{4\pi \left(\sum_i r_i\right)^2 k} \, dV \quad , \qquad \ldots (10)$$

where:

D_γ = dose rate (roentgens/hour)
S_v = gamma-ray source strength (Mev/cc-sec)
B_r = dose buildup factor
μ_i = linear absorption coefficient in the i^{th} absorbing medium (cm^{-1})
r_i = distance traveled in the i^{th} absorbing medium (cm)

TABLE I

BSR CORE GAMMA-RAY SOURCE STRENGTH

Gamma-Ray Energy (Mev)	Source Strength $\frac{\text{Mev} \times 10^{-5}}{\text{cc-sec-watt}}$					
	U^{235}(n, f and n, γ)	Al(n, γ)	H(n, γ)	$Al^{28} \rightarrow \gamma$	Fission Products	Total
0.30	3.34	—	—	—	—	3.34
0.43	—	—	—	—	1.68	1.68
1.00	7.80	0.0311	—	—	5.80	13.63
1.80	6.41	—	—	0.588	3.73	10.73
2.23	—	—	1.86	—	—	1.86
2.40	2.35	0.189	—	—	1.11	3.65
3.00	3.22	0.395	—	—	1.28	4.89
3.70	1.47	0.213	—	—	0.463	2.14
4.25	0.805	0.272	—	—	0.212	1.29
4.75	0.706	0.242	—	—	0.122	1.07
5.20	0.138	0.892	—	—	0.0585	0.286
5.60	0.217	0.150	—	—	0.0370	0.404
6.20	0.265	0.107	—	—	—	0.372
6.80	0.0784	0.0620	—	—	—	0.140
7.20	0.0553	—	—	—	—	0.0553
7.72	0.0540	0.866	—	—	—	0.925
8.50	0.0451	—	—	—	—	0.0451
9.50	0.0184	—	—	—	—	0.0184

k = factor converting energy flux to dose rate[28] for the gamma rays being considered (Mev/cm^2-sec-roentgen/hr).

Let us consider the BSR core source as a uniform homogeneous volume equivalent right-circular cylinder viewed from the side with the radius and height equal to 21.5 cm and 61.0 cm, respectively. The source geometry is shown in Fig. 1.

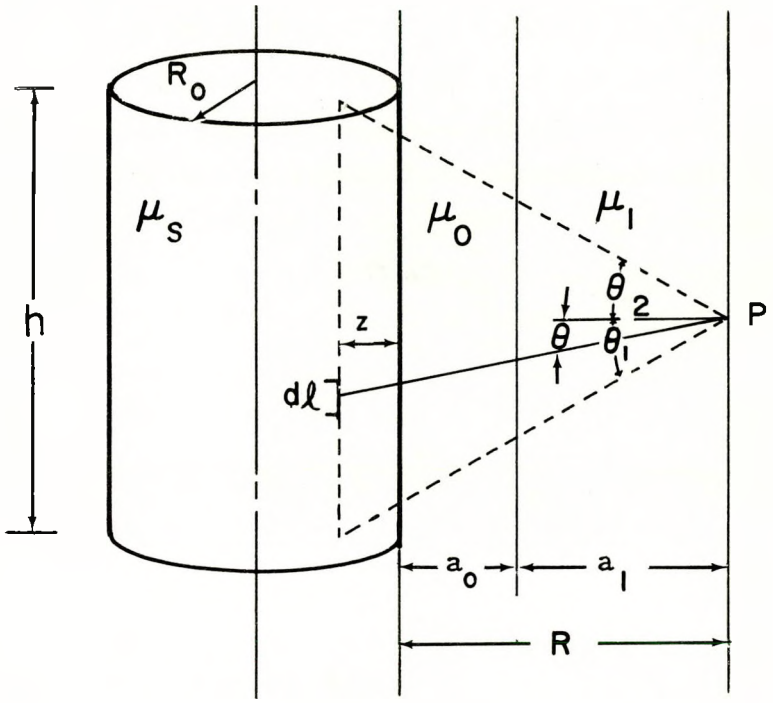

Fig. 1. Geometry for Uniform Cylindrical Source With Slab Shield

It has been shown[17] that a source of this geometry may be approximated by a line source having a source intensity per unit length equal to

$$S_\ell = \pi R_o^2 S_v \qquad \ldots(11)$$

provided that the line source is placed within the cylinder so as to correctly account for the self-absorption of the cylinder. Thus, Eq. (10) may be written as

$$D_\gamma = \int_\ell \frac{\pi R_o^2 S_v B_r e^{-(\mu_s z + \mu a)\sec\theta}}{4\pi \left[(z + R)\sec\theta\right]^2 k} d\ell \qquad \ldots(12)$$

where:

μ_s = linear absorption coefficient in the core (cm^{-1})

z = effective self-attenuation distance (cm)

R = distance from the surface of the cylinder to the detector (cm)

R_o = radius of the cylindrical source (cm)

$\mu a = \sum_{i=0}^{n} \mu_i a_i$

a_i = thickness of the i^{th} shield region (cm) .

Representing the dose buildup factor by the expression

$$B_r(\mu r) = Ae^{\alpha(\mu r)}$$

and substituting

$$d\ell = (R + z) \sec^2 \theta \, d\theta$$

Eq. (12) becomes

$$D_\gamma = \int_{\theta_1}^{\theta_2} \frac{R_o^2 S_v Ae^{-(\mu_s z + \mu a)(1-\alpha)\sec\theta}}{4(R + z) k} d\theta \qquad \ldots(13)$$

or, when $\theta = -\theta_1 = \theta_2$

$$D = \frac{A S_v R_o^2}{2(R + z) k} F\left[\theta, b(1-\alpha)\right] \qquad \ldots(14)$$

where

$$b = (\mu_s z + \mu a)$$

and

$$F\left[\theta, b(1-\alpha)\right] = \int_0^{\theta} e^{-b(1-\alpha)\sec\theta} \, d\theta \, .$$

Using the curves obtained by Foderaro and Obenshain[17] from an empirical fit to the exact calculations by Taylor and Obenshain,[18] the approximate location of the equivalent line source, i.e., the value of z, may be easily determined.

The values for A and α must be determined each time Eq. (14) is evaluated, i.e., each time the energy or shield thickness is changed. This is most easily accomplished by using a semi-logarithmic plot of the buildup factor as a function of the penetration, in mean free paths, to graphically obtain the best fit to B_r in the region of concern. By carefully choosing the values for A and α which give the best fit to the buildup factor data over an interval from b to (b + x), where $x \geq 3$ mean free paths, excellent agreement to an exact representation of the data may be obtained.

The contribution made by the core radiations to the dose rate in the water shield at any distance from the core may thus be evaluated by using Eq. (14).

B. SHIELD CAPTURE GAMMA RAYS

The dose rate at a position P (see Fig. 2) in the shield due to capture gamma rays produced in any shield region t is described by the expression

$$D_\gamma = \int_{V_t} \frac{\phi_n(x) \, \Sigma_a \eta E_\gamma B_r(\mu r) \, e^{-\mu r}}{4\pi r^2 k} \, dV_t \qquad \ldots(15)$$

where :

$\phi_n(x)$ = thermal neutron flux in the region t $\left(\frac{\text{neutrons}}{\text{cm}^2\text{-sec}}\right)$

Σ_a = macroscopic thermal neutron absorption coefficient in the region t (cm^{-1})

η = the number of gamma rays of a given energy (or within a given energy interval) created per neutron capture

E_γ = energy of capture gamma ray being considered (Mev)

$$\mu r = \sum_{i=1}^{n} \mu_i r_i$$

and the remaining terms are as defined in Section IV. A above and by Fig. 2. Using the notation in Fig. 2, Eq. (15) may be rewritten in slab geometry as

$$D_\gamma(\text{slab}) = \frac{\Sigma_a \eta E_\gamma}{2k} \int_t^0 \phi_n(x)\, dx \int_0^{\pi/2} B_r\left(\frac{\mu a + \mu_t t - \mu_t x}{\cos\theta}\right) e^{-\left(\frac{\mu a + \mu_t t - \mu_t x}{\cos\theta}\right)} \tan\theta\, d\theta \qquad \ldots(16)$$

where

$$\mu a = \sum_{i=1}^{n} \mu_i a_i$$

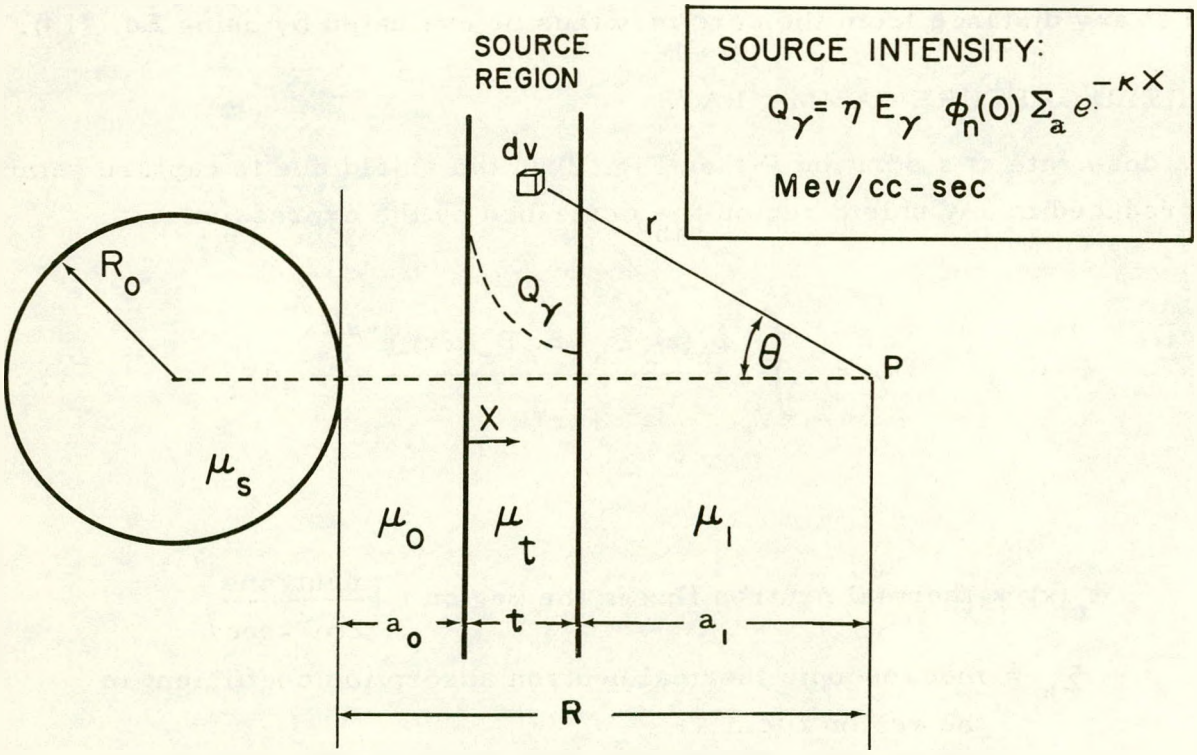

Fig. 2. Geometry for Exponential Slab Source With Slab Shield

This expression is essentially an integration over a series of infinite plane sources of thickness dx. Since this source is more appropriately represented by a sphere than by an infinite slab, the well known transformation from an infinite plane source to a spherical shell source[19] will be used and the integration carried out over the shells. Thus, referring again to Fig. 2.

$$D_\gamma(\text{shell}) = \frac{R_o + a_o + x}{R_o + R} D_\gamma(\text{plane}) \qquad \ldots(17)$$

which, when substituted into Eq. (16) gives

$$D_\gamma(\text{sphere}) = \frac{\Sigma_a \eta E_\gamma}{2k} \int_t^0 \frac{\phi_n(x)\,(R_o + a_o + x)}{R_o + R}\, dx$$

$$\cdot \int_0^{\pi/2} B_r\left(\frac{\mu a + \mu_t t - \mu_t x}{\cos\theta}\right) e^{-\left(\frac{\mu a + \mu_t t - \mu_t x}{\cos\theta}\right)} \tan\theta \; d\theta \; . \qquad \ldots(18)$$

In order to simplify the integration, the experimentally measured[1] thermal neutron flux was replotted by multiplying ϕ_n (measured) by the ratio

$$\frac{R_o + a_o + x}{R_o + R} \; .$$

The resultant curve was then represented by a series of exponentials, such that in the region t

$$\frac{\phi_n(x)\,(R_o + a_o + x)}{R_o + R} \cong \phi_n'(o)\, e^{-\kappa_t x} \qquad \ldots(19)$$

where

$$\phi_n'(o) = \frac{R_o + a_o}{R_o + R}\ \phi_n(o)$$

and κ_t is a constant chosen so as to give the best fit to the replotted flux in the region t. Substituting Eq. (19) into Eq. (18)

$$D_\gamma = \frac{\Sigma_a \eta E_\gamma \phi_n'(o)}{2k} \int_t^0 e^{-\kappa_t x}\, dx \int_0^{\pi/2} B_r\left(\frac{\mu a+\mu_t t-\mu_t x}{\cos\theta}\right) e^{-\left(\frac{\mu a+\mu_t t-\mu_t x}{\cos\theta}\right)} \tan\theta\ d\theta\ . \quad \ldots(20)$$

For a geometry such as this, it has been found[29] that a polynomial type representation to the dose buildup factor will lead to an exact solution. Replacing B_r in Eq. (20) by a quadratic of the form

$$B_r(\mu r) = 1 + C_1(\mu r) + C_2(\mu r)^2$$

and integrating the resulting expression, the dose rate becomes

$$D_\gamma = \frac{\phi_n'(0)\ \Sigma_a \eta E_\gamma e^{-\kappa_t t}}{2k\kappa_t} \left\{ e^{\kappa_t t} E_1(\mu_t t + \mu a) - E_1(\mu a) \right.$$

$$+ e^{-\frac{\kappa_t}{\mu_t}\mu a}\left[E_1\left[\left(1-\frac{\kappa_t}{\mu_t}\right)\mu a\right] - E_1\left[\left(1-\frac{\kappa_t}{\mu_t}\right)\left(\mu_t t+\mu a\right)\right]\right]$$

$$+ C_1 \frac{\kappa_t e^{\kappa_t t}}{\kappa_t-\mu_t} e^{-\mu a}\left[e^{-\mu_t t} - e^{\kappa_t t}\right]$$

$$\left. + C_2 \frac{\kappa_t e^{\kappa_t t}}{\kappa_t-\mu_t} e^{-\mu a}\left[\mu_t t\, e^{-\mu_t t} + \left(\mu a + \frac{\kappa_t-2\mu_t}{\kappa_t-\mu_t}\right)\left(e^{-\mu_t t} - e^{-\kappa_t t}\right)\right]\right\} \quad \ldots(21)$$

where

$$E_1(y) = \int_1^\infty \frac{e^{-yt}}{t}\, dt \ .$$

$E_1(y)$ can be calculated by means of the formula

$$E_n(y) = \frac{e^{-y}}{y + n - 1 + f_{n-1}(y)} \qquad \ldots (22)$$

where $f_n(y)$ for $y > 0$ has been evaluated by Morrison[20] and is shown in Fig. 3. Values of $f_1(y)$ for $y < 0$ had to be calculated for the purpose of this study as they had not been tabulated. These values are shown in Fig. 4.

Substituting Eq. (22) into Eq. (21) and rearranging the terms,

$$D_\gamma = \frac{\phi_n'(0)\Sigma_a \eta E_\gamma e^{-P}}{2k\kappa_t} \left\{ \frac{1}{P + f_o(P)} - \frac{1}{(1-\beta)P + f_o\left[(1-\beta)P\right]} \right.$$
$$+ \frac{\beta}{\beta-1}\left[C_1 + C_2\left(P + \frac{\beta-2}{\beta-1}\right)\right] + e^{(1-\beta)\mu_t t}\left[\frac{1}{(1-\beta)\mu a + f_o\left[(1-\beta)\mu a\right]}\right.$$
$$\left.\left. - \frac{1}{\mu a + f_o(\mu a)} - \frac{\beta}{\beta-1}\left[C_1 + C_2\left(\mu a + \frac{\beta-2}{\beta-1}\right)\right]\right]\right\} \qquad \ldots (23)$$

where:

$$\beta = \frac{\kappa_t}{\mu_t}$$

$$P = \mu_t t + \mu a \ .$$

22

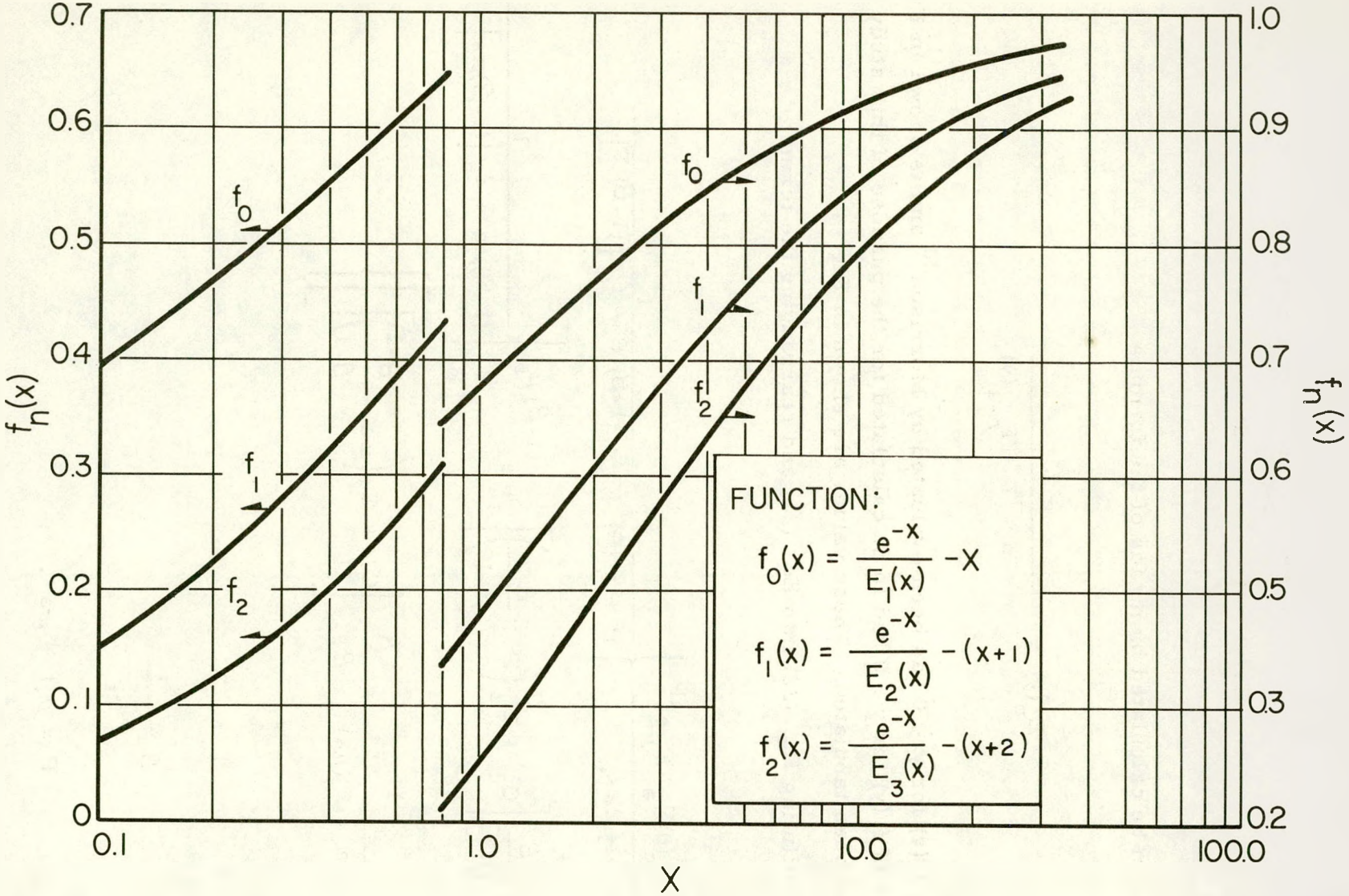

Fig. 3. The Functions $f_o(x)$, $f_1(x)$, $f_2(x)$

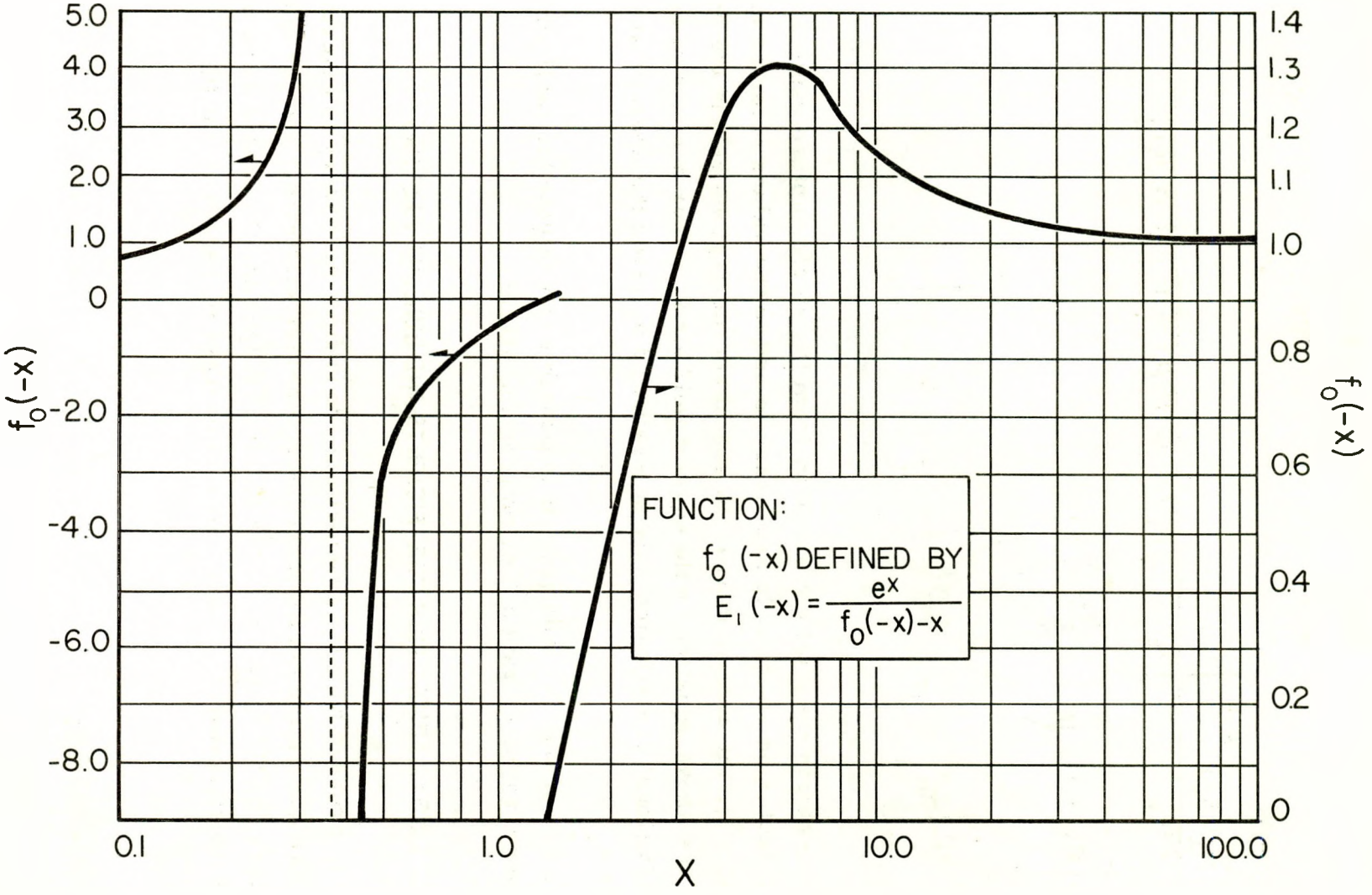

Fig. 4. The Function $f_0(-x)$

Similarly, it can be shown that when $\mu a = 0$, i.e., no shield, the gamma dose rate becomes

$$D_\gamma = \frac{\phi'_n(0)\,\Sigma_a \eta E_\gamma e^{-\mu_t t}}{2k\kappa_t}\left\{\frac{1}{\mu_t t + f_o(\mu_t t)} - \frac{1}{(1-\beta)\mu_t t + f_o\left[(1-\beta)\mu_t t\right]}\right.$$

$$+ \frac{\beta}{\beta_{-1}}\left[C_1 + C_2\left(\mu_t t + \frac{\beta_{-2}}{\beta_{-1}}\right)\right]$$

$$\left. + e^{(1-\beta)\mu_t t}\left[\ln\left|\frac{1}{1-\beta}\right| - \frac{\beta}{\beta_{-1}}\left(C_1 + C_2\,\frac{\beta_{-2}}{\beta_{-1}}\right)\right]\right\} \qquad \ldots(24)$$

In order to obtain the total contribution from the shield capture gamma rays at a given detector position, it is necessary to add to the values obtained using Eq. (23) and (24), the contribution from shield source regions behind the detector. Since the above equations hold equally well for κ_t either positive of negative, this additional contribution may be evaluated by using the appropriate value and sign for κ_t.

Thus, by use of Eq. (23) and (24), it is possible to evaluate the total shield capture gamma-ray dose rate at any point in the shield.

V. LINEAR ABSORPTION COEFFICIENTS AND BUILDUP FACTORS

In order to proceed with the calculations, it is first necessary to determine both the linear absorption coefficients (less coherent scattering) and the dose buildup factors for the core and water shield. Values for the shield were obtained from the literature[7, 21] and are summarized in Tables II and III.

TABLE II

LINEAR ABSORPTION COEFFICIENT FOR WATER

E_γ (Mev)	μ (cm^{-1})
0.5	0.0967
0.8	0.0786
1.0	0.0706
1.5	0.0576
2.0	0.0493
3.0	0.0396
4.0	0.0339
5.0	0.0302
6.0	0.0277
8.0	0.0242
10.0	0.0221

TABLE III

DOSE BUILDUP FACTOR FOR WATER-POINT ISOTROPIC SOURCE

	Buildup Factor						
E(Mev)	(μr=1)	(μr=2)	(μr=4)	(μr=7)	(μr=10)	(μr=15)	(μr=20)
0.5	2.52	5.14	14.3	38.8	77.6	178.	334.
1.0	2.13	3.71	7.68	16.2	27.1	50.4	82.2
2.0	1.83	2.77	4.88	8.46	12.4	19.5	27.7
3.0	1.69	2.42	3.91	6.23	8.63	12.8	17.0
4.0	1.58	2.17	3.34	5.13	6.94	9.97	12.9
6.0	1.46	1.91	2.76	3.99	5.18	7.09	8.85
8.0	1.38	1.74	2.40	3.34	4.25	5.66	6.95
10.0	1.33	1.63	2.19	2.97	3.72	4.90	5.98

In computing the buildup factor for the core, the method suggested by Goldstein and Wilkins[7] was used. In this method the absorption coefficient per electron, μ_e, for a homogeneous mixture is defined by:

$$\mu_e = \sum_i \beta_i \mu_i \qquad \ldots(25)$$

where μ_i is the corresponding electron absorption coefficient (less coherent scattering) for the i^{th} element in the mixture and β_i is the electron fraction, given by

$$\beta_i = \frac{a_i z_i}{A_i} \Bigg/ \sum_j \frac{a_j z_j}{A_j} \quad . \qquad \ldots(26)$$

Here, a_i is the weight fraction, A_i the atomic weight, and z_i the number of electrons per atom.

For the core composition listed in Section I, we have:

Element	Weight Fraction (a_i)	Electron Fraction (β_i)
hydrogen	0.0381	0.0749
oxygen	0.3020	0.2991
aluminum	0.6375	0.6086
uranium	0.0224	0.0174

The values for the absorption coefficient per electron in the core, calculated from Eq. (25), are plotted in Fig. 5. The shape of this curve was then compared with those of the single elements with the result that for energies above 2 Mev the curve could best be represented by the element for which Z = 13, aluminum, and for energies below 2 Mev by the element for which Z = 26, iron. Consequently, the aluminum buildup factor was used to represent the buildup factor for the core in calculations involving source energies in excess of 2 Mev and the buildup factor for iron was used in calculations involving energies below 2 Mev.

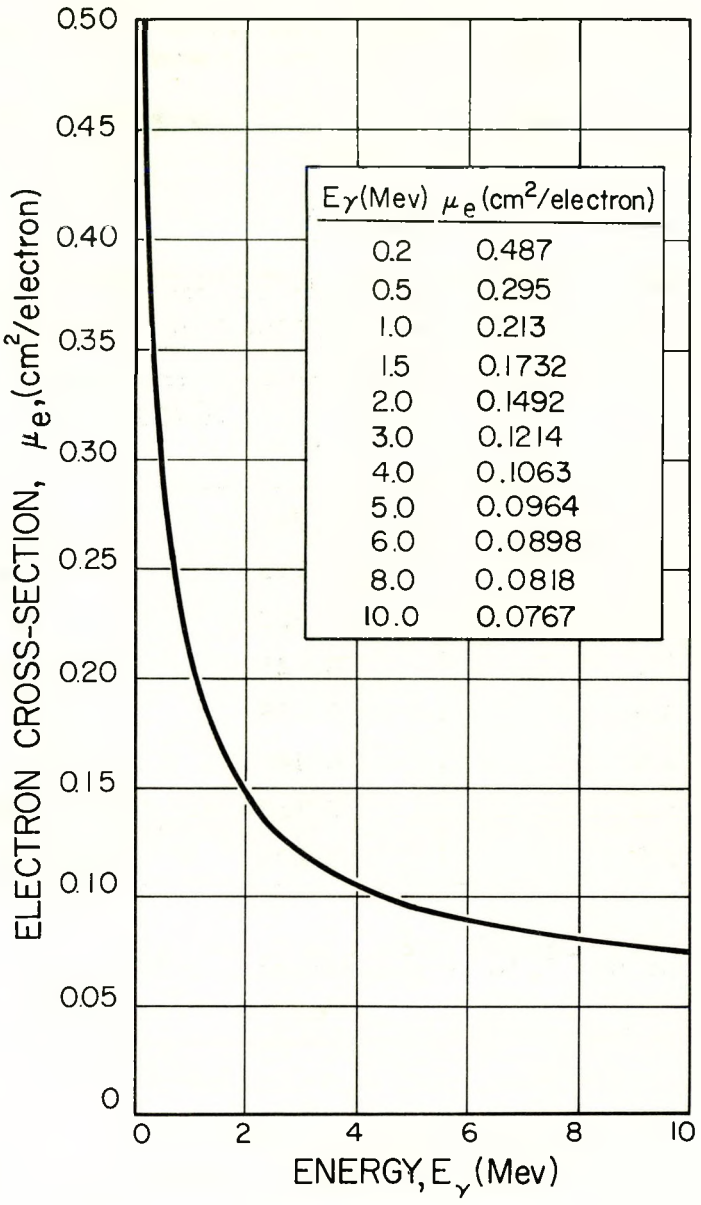

Fig. 5. Calculated Electron Cross Section for the BSR Core

The values of the constants A and α, necessary for the evaluation of Eq. (14), were determined from semi-logarithmic plots of the dose buildup factors for iron, aluminum and water (See Section IV A). The dose buildup factor for water was also fitted to a quadratic and the constants C_1 and C_2, necessary for the evaluation

of Eq. (23) and Eq. (24), were obtained. The values of C_1 and C_2 are listed in Table IV.

TABLE IV

CONSTANTS FOR QUADRATIC REPRESENTATION TO DOSE BUILDUP FACTOR FOR WATER

E_γ (Mev)	Constants	
	C_1	C_2
0.5	0.780	0.715
1.0	1.115	0.142
2.0	0.900	0.0226
3.0	0.725	0.00385
4.0	0.595	-0.00010
6.0	0.446	-0.0030
8.0	0.360	-0.0028
10.0	0.299	-0.0026

The values of μ_s (in cm^{-1}) to be substituted into Eq. (14) were obtained by using the relation

$$\mu_s = \rho_s \sum_i \left(\frac{\mu}{\rho}\right)_i a_i \qquad \ldots (27)$$

where μ_s is the average density of the core, = 1.734 gm/cc, and $\left(\frac{\mu}{\rho}\right)_i$ is the mass absorption coefficient (less coherent scattering) in cm^2/gm of the i^{th} element. A curve of μ_s as a function of gamma-ray energy is plotted in Fig. 6.

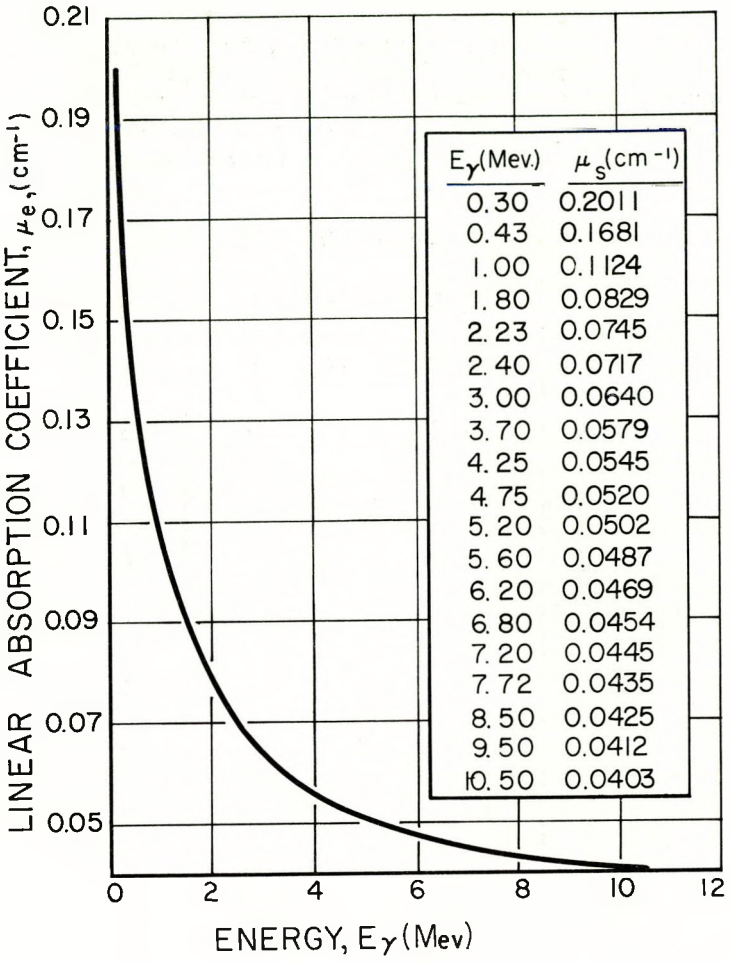

Fig. 6. Calculated Linear Absorption Cross Section for the BSR Core

VI. CALCULATION OF THE DOSE RATE

Using the data obtained in the previous section, Eq. (14) was evaluated to obtain the dose rate in the water shield due to core gamma rays. Values of the dose rate from 25 to 700 cm were obtained using a buildup factor assuming all of the penetration was in the water. The dose rate out to 75 cm was also determined using a buildup factor which assumed all the penetration in the core material. The results are listed in Table V.

TABLE V

DOSE RATE DUE TO CORE GAMMA RAYS

Water Thickness (cm)	Calculated Dose Rate* (r/hr-watt)	
0	7.49×10^{1} †	—
25	6.57×10^{0} †	9.65×10^{0}
50	1.09×10^{0} †	1.48×10^{0}
75	2.39×10^{-1} †	3.13×10^{-1}
100	—	7.32×10^{-2}
150	—	6.72×10^{-3}
200	—	8.37×10^{-4}
250	—	1.62×10^{-4}
300	—	2.90×10^{-5}
400	—	1.20×10^{-6}
500	—	6.85×10^{-8}
600	—	4.44×10^{-9}
700	—	2.68×10^{-10}

The dose rate out to 300 cm from the core, due to hydrogen capture gamma rays originating in the water shield, was evaluated using Eq. (23) and Eq. (24). Evaluation beyond 300 cm was unnecessary, as the contribution from this source to the total dose rate in the shield beyond this point is less than 1 per cent. The total capture gamma-ray dose rate thus obtained is listed in Table VI.

The total gamma-ray dose rate in the water shield is listed in Table VII along with the experimental values obtained at the BSR.

*Unless noted, calculated values were determined using the dose buildup factor for water.

† Values obtained using dose buildup factor for core.

VII. COMPARISON OF CALCULATED AND MEASURED VALUES

The ratio of the calculated to the measured values for the gamma-ray dose rate in the BSR shield is listed in Table VIII. The table indicates that for shield thicknesses up to 50 cm the ratio is more consistent for the values obtained by using the dose buildup factor for the core.

TABLE VI

DOSE RATE DUE TO SHIELD CAPTURE GAMMA RAYS

Water Thickness (cm)	Dose Rate (r/hr watt)
0	7.07
25	1.14
50	1.83×10^{-1}
75	3.84×10^{-2}
100	9.18×10^{-3}
150	6.24×10^{-4}
200	4.79×10^{-5}
250	3.92×10^{-6}
300	3.23×10^{-7}

TABLE VII

TOTAL CALCULATED AND MEASURED DOSE RATES IN WATER SHIELD

Water Thickness (cm)	Total Dose Rate (r/hr-watt)		
	Calculated*		Measured at BSR
0	8.20×10^{1} †	—	7.00×10^{1}
25	7.71×10^{0} †	1.08×10^{1}	5.20×10^{0}
50	1.27×10^{0} †	1.66×10^{0}	1.03×10^{0}
75	2.77×10^{-1} †	3.51×10^{-1}	2.37×10^{-1}
100	—	8.24×10^{-2}	$6.2[illegible] \times 10^{-2}$
150	—	7.34×10^{-3}	$5.[illegible] \times 10^{-3}$
200	—	8.85×10^{-4}	$6.[illegible] \times 10^{-4}$
250	—	1.66×10^{-4}	1.15×10^{-4}
300	—	2.93×10^{-5}	2.21×10^{-5}
400	—	1.20×10^{-6}	1.09×10^{-6}
500	—	6.85×10^{-8}	6.60×10^{-8}
600	—	4.44×10^{-9}	4.15×10^{-9}
700	—	2.68×10^{-10}	2.62×10^{-10}

*Unless noted, calculated values were determined using the dose buildup factor for water.

† Values obtained using dose buildup factor for core.

The average ratio of the calculated dose rates to those measured at the BSR (from Table VIII) is 1.25 and the average deviation from this value is only 11.0 per cent, while the maximum deviation is 18.4 per cent.

TABLE VIII

RATIO OF CALCULATED TO MEASURED DOSE RATES

Water Thickness (cm)	Ratio*	
0	1.17 †	—
25	1.48 †	2.08
50	1.23 †	1.62
75	1.17 †	1.48
100	—	1.33
150	—	1.29
200	—	1.31
250	—	1.44
300	—	1.33
400	—	1.10
500	—	1.04
600	—	1.07
700	—	1.02

*Unless noted, the ratio uses values obtained using the dose build-up factor for water.
†Ratios obtained with calculated values using dose buildup factor for core.

VIII. DISCUSSION

In order to better interpret the results of this study, a discussion of the more important assumptions made and their effect on the results obtained is appropriate.

A. UNIFORM POWER DENSITY AND AVERAGE THERMAL NEUTRON FLUX

In determining the core source spectra and intensity, two of the more important assumptions made were that the power density in the core was uniform and that the average thermal neutron flux in the core could be represented by the average thermal neutron flux in the fuel. The former caused the calculated values of the dose rate in the shield to be slightly high, thus to some extent explaining the consistently high ratio of the calculated to measured dose rates shown in Table VIII. The latter assumption caused the contribution to the source intensity from the aluminum and core hydrogen capture gamma rays to be slightly low in comparison to the prompt and delayed gamma rays from the fuel. This is possibly the explanation for the consistently lower values obtained for the ratio of the calculated to measured dose rates at distances beyond 300 cm from the core, where the major contribution to the dose rate is from the 7.72 Mev aluminum capture gamma rays. Table I indicates that any effect upon the dose rate in the vicinity of the core due to small variations in either the core hydrogen or aluminum capture gamma-ray intensity will be negligible.

It should be noted that the assumption that the average thermal neutron flux in the core can be adequately represented by the average thermal neutron flux in the fuel is not equally valid for all reactor designs. Though the effect of this assumption is small in the BSR it can be of considerable importance in other reactors. This is due primarily to the fact that the ratio of the average thermal neutron flux in materials outside of the fuel region to the average thermal neutron flux in the fuel will become larger as the fuel region thickness or moderator region thickness is increased. Thus, by using this assumption in calculations where either the moderator or fuel region thickness is relatively large, the capture gamma-ray intensity calculated for materials outside of the fuel region may be considerably underestimated.

B. FISSION PRODUCT GAMMA-RAY SPECTRUM

Another possible source of error arises from an uncertainty in the fission product gamma-ray spectrum. The results of a recent experiment, performed at ORNL by Peelle, Zobel, and Love, [5] to measure the short-lived fission product gamma rays provided the basis for the spectrum used in this study. The measurements were performed using a multiple-crystal gamma-ray spectrometer and a circulating fuel belt with transit times between 1.2 and 2.5 seconds.

The spectrum of the gamma radiation was measured approximately 3 hours after the beginning of the activation of the fuel loop, thus representing about a 1-hour fuel irradiation.

Since the fuel elements in the BSR, at the time the measurements[1] were performed, were initially "cold", it was assumed that the spectrum reported by Peelle, Zobel, and Love was directly applicable to this analysis without further correction for longer or shorter irradiation. Bertini, et al.[6], have estimated that after the approximate 1 hour irradiation 86 per cent of the saturation activity of the circulating fuel belt was measured. Thus, any error in the results presented here, which arise from this assumption, is small. For example, a 30 per cent decrease in the intensity of the fission product spectrum will change the average ratio of the measured to calculated dose rates by only 4.2 per cent.

C. DOSE BUILDUP FACTORS

The buildup factor for the core was obtained by using the "effective Z" method suggested by Goldstein and Wilkins.[7] The element for which Z = 26, iron, was found to give the best representation for the core buildup factor for energies below 2 Mev and the element for which Z = 13, aluminum, was found to give the best representation for energies above 2 Mev. Although no single element by itself could be found to represent the core over the entire energy range considered, it is not expected that the use of a single element to represent the core buildup factor will significantly affect the results. This is due primarily to the fact that, over the range of penetrations in which the core buildup factor was used, at least 60 per cent of the dose rate was caused by gamma rays of energies less than 2 Mev. Furthermore, the difference in the buildup factor for iron and aluminum is less than 10 per cent for energies above 2 Mev and for penetrations of less than seven mean free paths (142 cm of water for 2 Mev gamma rays).

The dose buildup factors used in this study were those calculated by Goldstein and Wilkins[7] for a point isotropic source in an infinite homogeneous medium. Only recently has the behavior of buildup factors in multi-region shields been investigated.[25, 26] However, at this time, the results of these investigations are not complete nor are they readily adaptable to the type of analysis presented here. Therefore, in the formula used to determine the dose rate in the water

shield, the buildup factor at any position in the shield was found by assuming that the entire penetration occurred in either the core or shield material.

At distances in close proximity to the core, where the low energy gamma rays constitute the major contribution to the dose rate, the results obtained using the buildup factors calculated by assuming the entire penetration in the water shield will constitute the upper limit, whereas using the buildup factors calculated by assuming all of the penetration in the core material will constitute the lower limit. From the results shown in Table VIII, it may be concluded that for distances of from 0 to 50 cm the dose buildup fáctor is best represented by assuming all of the penetration in the core material, and beyond 50 cm by assuming all of the penetration in the water shield.

At considerable distances from the core, beyond approximately 300 cm, where the 7.72 Mev aluminum capture gamma rays form the major contribution to the dose rate, the assumption that all of the penetration occurs in the water shield will give a lower limit to the results. This may be readily seen by observing that for 7.72 Mev gamma-ray penetration in excess of six mean free paths, (244 cm of water), the dose buildup factor for the core (Z_{eff} = 13) is greater than the dose buildup factor for the water shield. Consequently, using the dose buildup factor for water beyond 300 cm will tend to slightly underestimate the calculated values of the dose rate. However, since the penetration in the water shield is so much greater than the penetration in the core material, the resultant error is expected to be quite small. At distances from 50 to 300 cm, no general conclusions of this type may be drawn.

In summary then, it may be concluded that, everything else being equal, the values of the ratio of the calculated to measured dose rates from 0 to 50 cm using the buildup factor for the core material and from approximately 300 to 700 cm using the buildup factor for water represent lower limits to the theoretically exact values.

D. GEOMETRY

The source geometry chosen to represent the BSR core was a right circular volume equivalent cylinder of finite length viewed from the side. The method

outlined in WAPD-TN-508[17] was used to evaluate the dose rate in the shield as a function of distance from this source. For values of $\frac{a}{R_o} > 10$, see Fig. 1, this method has been found to yield errors of less than ±10 per cent; whereas for values of $\frac{a}{R_o} < 10$ the errors have been found to be equal to or less than +40 per cent and -5 per cent. Thus, since a value of 21.5 cm was used for the radius of the cylinder, this method of calculation may introduce errors in the calculated dose rate at positions beyond 200 cm from the core of ±10 per cent and errors at positions of 200 cm or less from the core of from +40 per cent to -5 per cent. These limits for the error indicate that the calculated values of the dose rate in close to the core can be higher than the values far out. Furthermore, the cylindrical model chosen to approximate the core geometry is expected to cause some additional error. However, since the thermal neutron flux in the core is not uniform but drops off at the core boundaries, the error introduced by this approximation is expected to be quite small.

E. SHIELD DENSITY

Throughout the analysis, the density of the water shield was assumed to be 1.0000 gm/cc. The table shown below gives the density of water in grams per milliliter as a function of temperature in °C.

TABLE IX

RELATIVE DENSITY OF WATER[27]

Temp. (° C)	Density (gm/ml)
4	1.00000
10	0.99973
20	0.99823
30	0.99567
40	0.99224
50	0.98807

Thus, the assumption that the shield density was 1.0000 gm/cc implies that the average temperature of the water shield was 4° C. At considerable distances from the core, the effect of small density changes due to higher temperatures becomes important. For example, assuming the water temperature was 30° C rather that 4° C, will increase the contribution to the dose rate at 700 cm from

the 7.72 Mev gamma rays by 7.4 per cent. Since 30° C rather than 4° C is a more realistic value to assume for the shield temperature at the time the measurements were performed, it may be concluded that, due to this effect, the calculated dose rate at considerable distances from the core may be low by as much as from 5 to 10 per cent.

IX. CONCLUSION

The discrepancies between the ratios of the calculated to measured values of the dose rates in the BSR shield may be attributed, for the most part, to the errors discussed in the preceding section; principally, to the error caused by assuming that the power distribution in the core is uniform, and by the method used to evaluate the dose rate from a shielded cylindrical source. However, for shielding calculations, the type of accuracy obtained in this study is probably more than adequate. Additional refinements of the method presented here will not necessarily produce better accuracy in shield calculations, since, for example, a two per cent error in the value of the linear absorption coefficient for a given shield material will yield an error of 35 per cent at a penetration of 15 mean free paths. For the water shield under consideration here, this penetration would correspond to a shield thickness of 610 cm for the 7.72-Mev aluminum capture gamma ray. Furthermore, since buildup factors have been extensively tabulated for infinite media and consequently are applicable only to the type of problem presented here, the effect of their use on finite shields (which are the usual type encountered in shielding problems) will be to introduce some additional error. The magnitude of this error has only recently been investigated.[22] For example, for a 1-Mev gamma-ray source in a water shield, a boundary at 16 mean free paths will reduce the dose rate from that calculated using infinite media data at the boundary by 17 per cent. For higher Z shield materials, the error is less.

It may be concluded then, that the approach of assuming a uniform power density in the core and representing the core thermal flux by the average thermal

flux in the fuel is (at least in this design) reasonable; and furthermore, that the gamma-ray energy spectra chosen and the formulae describing their attenuation will yield results which, for shielding analyses, are more than adequate. When dealing with heat generation problems where, for example, the shield coolant system capacity or stress analysis is involved, the consistency of the ratio of the calculated to measured dose rates indicates that this method will also yield results which are quite adequate.

REFERENCES

1. F. C. Maienschein, et al., "Attenuation by Water of Radiations From a Swimming Pool Type Reactor," ORNL-1891 (Sept. 19, 1955).
2. B. B. Kinsey, R. C. Hanna, and D. Van Patter, "Gamma-Rays Produced in the Fission of U^{235}," Canadian Journal of Research, 26A, 79-98 (1948).
3. M. Deutsch and H. Rotblat, "Investigation of Fission Gamma-Rays," AECD-3179 (Nov. 13, 1944).
4. R. L. Gamble, "Prompt Fission Gamma-Rays from Uranium 235," Reactor Shielding Information Meeting, May 12-13, 1955, Engineer Research and Development Laboratories, Fort Belvoir, Virginia, WASH-292 (Pt. 3) (Sept. 1955).
5. R. W. Peelle, W. Zobel, and T. A. Love, "ANP Annual Progress Report, Sept. 10, 1956," ORNL-2081, p 91-102.
6. H. W. Bertini, C. M. Copenhaver, A. M. Perry, and R. B. Stevenson, ORNL-2113 (Sept. 17, 1956),
7. Herbert Goldstein and J. Ernest Wilkins, Jr., "Calculations of the Penetrations of Gamma Rays," NYO-3075 (June 30, 1954).
8. W. M. Breazeale, "The New Bulk Shielding Facility at Oak Ridge National Laboratory," ORNL-991 (May 8, 1951).
9. F. C. Maienschein and R. C. Cochran, "Prompt Fission Gamma-Rays," Paper Presented at the Reactor Shielding Information Meeting, Chicago, Ill., Nov. 12-13, 1953.
10. F. C. Maienschein, "Chart Showing Current Values for the Distribution of Energy Released by the Fission of U^{235} Induced by Thermal Neutrons," CF-56-10-9, (October 3, 1956.)
11. "The Reactor Handbook, Vol. I, Physics" AECD-3645 (Mar. 1955).
12. R. E. Bell and L. G. Elliott, "Gamma-Rays From the Reaction H^1 $(n,\gamma)D^2$ and the Binding Energy of the Deuteron," Phys. Rev. 79, 282-85 (1950).
13. B. B. Kinsey, G. A. Bartholomew, and W. H. Walker, "Neutron Capture Gamma-Rays From Fluorine, Sodium, Magnesium, Aluminum, and Silicon," Phys. Rev. 83, 519-534 (1951).
14. T. H. Braid, "Neutron-Capture Gamma-Rays From Various Elements," Phys. Rev. 102, 1109-1123 (1956).

15. J. M. Hollander, I. Perlman, and G. T. Seaborg, "Table of Isotopes," Rev. Mod. Phys., 25, 469-651 (April, 1953).
16. K. Way, and E. P. Wigner "Radiation From Fission Products," MDDC-48 (June 14, 1946).
17. A. Foderaro and F. E. Obenshain, "Fluxes From Regular Geometric Sources," WAPD-TN-508, (June, 1955).
18. J. J. Taylor and F. E. Obenshain, "Flux From Homogeneous Cylinders Containing Uniform Source Distributions," WAPD-RM-213 (Dec. 7, 1953).
19. Samuel Glasstone, "Principles of Nuclear Reactor Engineering," p 593, Van Nostrand, New York (1955).
20. R. S. Mulliken, P. Morrison and Associates, CL-697 (May, 1954), Classified.
21. Gladys R. White, "X-Ray Attenuation Coefficients From 10 Kev to 100 Mev," NBS-1003 (May 13, 1952).
22. M. J. Berger and J. Doggett, "Reflection and Transmission of Gamma Radiation by Barriers: Semianalytic Monte Carlo Calculation," Journal of Research of the National Bureau of Standards, 56, 89-98 (Feb. 1956).
23. H. W. Bertini, C. M. Copenhaver, H. C. Claiborne and T. Fowler, "Comparison of Calculated vs Measured Gamma-Ray Heating in the Bulk Shielding Facility," CF 56-11-36, (November 12, 1956).
24. D. J Hughes and J. A. Harvey, "Heavy Element Cross Sections Presented at Geneva, August, 1955," Addendum to BNL-325, (July 15, 1955).
25. S. Auslender, "A Monte Carlo Study of the Gamma-Ray Energy Flux, Dose Rate, and Buildup Factors in a Lead-Water Slab Shield of Finite Thickness," ORNL-2194 (January 29, 1957).
26. M. H. Kalos, NDC of A, "Some Theoretical Methods and Results in Gamma Ray and Neutron Shielding," Proceedings of the Shielding Symposium Held at the U.S. Naval Radiological Defense Laboratory October 17-19, 1956, USNRDL Reviews and Lectures No. 29, Vol. I, (February 1, 1957).
27. "Handbook of Chemistry and Physics," 31st Edition, 1949. Chemical Rubber Company, Cleveland, Ohio.
28. Theodore Rockwell III, "Reactor Shielding Design Manual," (Fig. 2.2) TID-7004 (March 1956.)
29. A. R. Vernon, "Analysis of the Biological Shield of the Sodium Reactor Experiment," NAA-SR-1949 (June 15, 1957.)